

PAPER

Direct spraying method for fabrication of paper-based microfluidic devices

To cite this article: Ning Liu *et al* 2017 *J. Micromech. Microeng.* **27** 104001

View the [article online](#) for updates and enhancements.

Related content

- [High-energy-density, all-solid-state microsupercapacitors with three-dimensional interdigital electrodes of carbon/polymer electrolyte composite](#)
Juan Pu, Xiaohong Wang, Tianyi Zhang et al.
- [Recent progress and performance evaluation for polyaniline/graphene nanocomposites as supercapacitor electrodes](#)
Mahmoud Moussa, Maher F El-Kady, Zhiheng Zhao et al.
- [Low-cost superior solid-state symmetric supercapacitors based on hematite nanocrystals](#)
Shaomin Peng, Lin Yu, Bang Lan et al.

Direct spraying method for fabrication of paper-based microfluidic devices

Ning Liu¹ , Jing Xu², Hong-Jie An¹, Dinh-Tuan Phan³,
Michinao Hashimoto⁴ and Wen Siang Lew^{1,5}

¹ School of Physical and Mathematical Sciences, Nanyang Technological University, 21 Nanyang Link, Singapore 637371, Singapore

² Herbert Gleiter Institute of Nanoscience, Nanjing University of Science and Technology, Nanjing, Jiangsu 210094, People's Republic of China

³ Department of Biomedical Engineering, National University of Singapore, Singapore 117574, Singapore

⁴ Pillar of Engineering Product Development, Singapore University of Technology and Design, 8 Somapah Road, Singapore 487372, Singapore

E-mail: wensiang@ntu.edu.sg

Received 31 May 2017, revised 24 July 2017

Accepted for publication 28 July 2017

Published 12 September 2017



Abstract

Direct spraying of hydrophobic materials is an affordable, easy-to-use and equipment-free method for fabrication of flexible microsensors, albeit not yet widely adopted. To explore its application potential, in this paper, we propose and demonstrate two novel hybrid methods to fabricate paper-based components. Firstly, through combing direct spraying with Parafilm embedding, a leak-free paper-based sample preconcentrator for fluorescence sensing was fabricated. The leak-free device worked on the principle of ion concentration polarization (ICP) effect, and achieved enhancement of fluorescent tracer by 220 folds on a paper substrate. Secondly, by using the sprayed hydrophobic patterns, paper-based micro-sized supercapacitors (mSCs) were fabricated. Vacuum filtration was used to deposit multi-wall carbon nanotubes (MWCNT)-dispersed solution on a porous substrate to form electrodes. A volumetric capacitance of 42.5 mF cm^{-3} at a current density of 2 mA cm^{-3} was obtained on the paper-based mSC. Our demonstrations have shown the versatility of direct spraying for the fabrication of integrative paper-based microfluidic devices.

Keywords: paper-based devices, microfluidics, ion concentration polarization, microfluidic sensor, fabrication

 Supplementary material for this article is available [online](#)

(Some figures may appear in colour only in the online journal)

1. Introduction

Low-cost and flexible microdevices are attracting much attention for their applications in biomedical engineering, energy generation and storage, customer electronics and industry sensors. In the past few decades, we have witnessed great progress in fabrication techniques of such devices. Using readily available materials and simple manufacturing procedures is a requirement for fabrication of economic, flexible devices.

To that end, papers and other porous substrates have offered remarkable advantages in cost and availability. A well-known example of application of papers is microfluidic paper-based analytical devices (μ PADs) for point-of-care testing, proposed by Whitesides and colleagues [1]. Owing to their simplicity and low price, μ PADs have been evidenced to have great potential in sensing applications, such as diagnostics, chemical analysis, and environmental monitoring [2]. The key step in fabricating μ PADs is to construct hydrophobic barriers on a paper substrate. To achieve this goal, various strategies have been introduced in the past years. Current fabrication methods

⁵ Author to whom any correspondence should be addressed.

for making μ PADs have been well-reviewed elsewhere [3–7]. In short, photolithography and wax printing are the most commonly used strategies. Each of these methods has its own advantages and limitations. Photolithography is the first technique used to fabricate μ PADs, where required consumables and facilities are generally expensive. Wax printing exploits commercialized wax printer to print wax on paper substrate, then utilizes hotplate to melt the wax to spread the wax into the paper [8]. Spreading of the wax is difficult to control during heating. Other fabrication methods were also reported, such as laser ablation [9], programmable paper cutting [10], flexography printing [11] and Parafilm embossing [12].

Direct spraying hydrophobic materials on porous substrates provides yet another low-cost, simple route to create hydrophobic barriers. However, reports about its application for fabrication of microdevices are limited to date. Matthew *et al* presented a simple method for fabricating gradient generator on glass slide using hydrophobic spray [13]. Firstly, they masked a rectangular region on a glass slide using a strip of tape. Then they applied hydrophobic spray on the glass slide surface. After 2 d drying, the tape mask was removed to expose hydrophilic stripe surrounded by hydrophobic boundary. Liu *et al* exploited hydrophobic spray method for fabricating plasma separator [14]. They sprayed a commercial water repellent product on a 3D-printed substrate to form hydrophobic barriers. Thara *et al* first introduced a concept of spraying method for fabrication of paper-based microfluidic devices [15]. They used a laser-cut iron mask to pattern hydrophobic regions and protect the remaining hydrophilic region in the paper. Then commercial lacquer was manually painted around the mask to make hydrophobic barrier. While these demonstrations have shown the potentials of direct spraying for low-cost, simple and fast patterning of materials, further improvements shall be needed for practical applications.

To extend the scope of direct spraying for a wider range of applications, we have developed two novel hybrid methods to fabricate paper-based devices. Both methods are featured with their simplicity of the fabrication process. We chose to fabricate two classes of devices: (1) ICP-based preconcentrator for fluorescence sensing and (2) microsized supercapacitors (mSCs) for constructing self-powered sensors. Very recently, ICP preconcentration method has been implemented on paper-based microfluidic devices to enhance sample concentration for fluorescence sensing [10, 16–20]. The paper-based ICP preconcentrator provided a promising solution to improve the detection sensitivity of μ PADs. However, most of the paper-based ICP preconcentrators were based on wax printing. Due to the limitation of wax printing mentioned above, fabrication of simple ICP preconcentrators has not been accessible to many researchers. As a representative example of flexible energy devices, paper-based microsized supercapacitors (mSCs) have spurred great interesting. There are many valuable propositions of using paper to build mSCs—cost, flexibility, and compatibility to various fabrication process. Importantly, a great potential application of paper-based mSCs lies in working as energy storage component for paper-based micro-devices, such as μ PADs. Ge *et al* first showed this potential by integrating paper SCs with photo-electrochemical (PEC) μ PADs as a photocurrents collection and storage units [21].

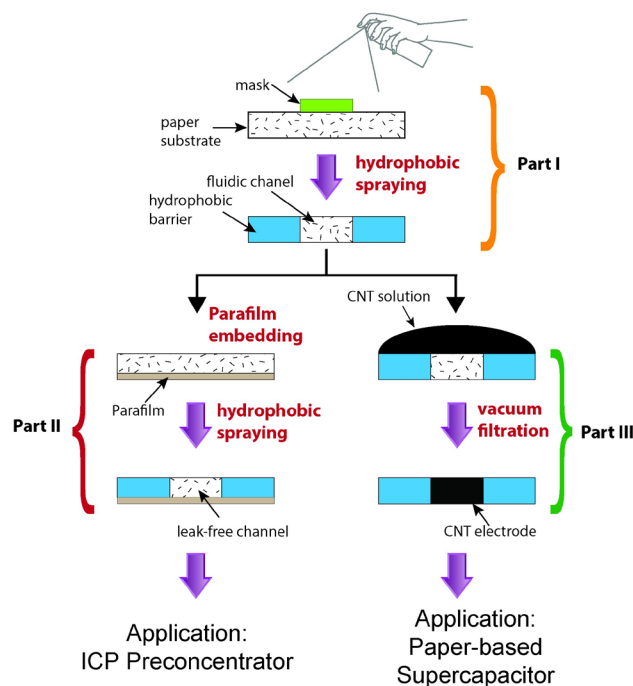


Figure 1. A schematic overview of the process described in this paper. Part I introduces a hydrophobic spraying method. Based on this simple fabrication method, part II and part III demonstrate the fabrication of leak-free paper channel and paper electrodes, respectively. The leak-free channel can be further applied to fabricate ICP preconcentrator for fluorescence sensing, and the paper electrodes can be used to construct paper-based microsupercapacitor.

To date, the number of reported in-plane paper-based mSCs is limited, and the approach we present here offers alternative, rapid route for fabrication of in-plane paper electrodes.

2. Experimental section

Both μ PADs fabrication and paper-based mSCs construction involve patterning desired structures on paper substrates. The ideal methods should minimize the total fabrication cost and time by simplifying manufacturing procedures and materials. The approach we present here starts with direct spraying, which is subsequently followed with another low-cost, bench-top method of microfabrication. Figure 1 illustrates the approach. Firstly, we explored non-expensive materials to create masks and obtained fluidic channels through one-step mask-assisted spraying (figure 1 part I). Based on this hydrophobic patterning method, we subsequently performed two hybrid techniques to fabricate leak-free paper channel and paper electrodes, respectively (figure 1, part II and part III). First, we fabricated an μ PAD to perform fluorescence sensing through direct spraying hydrophobic patterning combining with Parafilm embedding. The Parafilm melted and penetrated into the filter paper and served as an isolation substrate to seal the paper bottom, which could greatly reduce contamination risk and increase operation flexibility. Experimental results have shown that a 220-fold preconcentration factor was achieved in the μ PAD. Second, we implemented vacuum filtration and deposited conductive carbon material onto the hydrophobic patterned paper substrate to fabricate paper

electrodes. Based on the paper electrodes, we fabricated a paper-based mSC through packing the interdigital electrodes with gel electrolyte. In contrast to previously reported in-plane paper-based mSCs fabrication methods, the combination of one-step spraying and vacuum filtration provided a simple path to fabricate interdigital electrodes. The good performance of the paper-based mSC was demonstrated through electrochemical characterization.

2.1. Direct spraying hydrophobic patterning

Whatman® filter paper with thickness of 180 μm was chosen as substrate for μPADs fabrication. A commercially available water repellent product (Neverwet®, NeverWet L.L.C.) was purchased from a local retail store and employed here as hydrophobic coating material. Acrylic plastic plates and common paperboard were used to fabricate spray masks. AutoCAD® software (Autodesk, San Rafael, CA, USA) was used to design mask patterns. Computer numerical control (CNC) milling equipment (Stepcraft® 420, Stepcraft CNC system, Germany) amounted with 500 μm diameter endmill was used to cut designed patterns on acrylic plates. To further reduce the fabrication cost, a craft cutter (Silhouette America, Inc., Silhouette Cameo®) was also used to cut designed masks on paperboard. Both the acrylic and paper masks were adopted in this work to demonstrate their feasibility for direct spray patterning.

Figure 2 schematically outlines the hydrophobic patterning process for paper-based microdevices. Firstly, the paper substrate was sandwiched between a mask and a piece of glass that provided a back support (figure 2(B)). Subsequently, the hydrophobic coating was manually sprayed onto the substrate to form hydrophobic barriers along the boundaries of the mask. After the spraying, the substrate was left in a place with good ventilation for 15 min for drying. Finally, the paper substrate was disassembled from the sandwiched structure and the patterned papers were ready to use. The feasibility of the fabricated fluidic device was demonstrated by the time sequential images of blue dye flowing through the channels (figure 3).

2.2. Fabrication and operation of leak-free paper-based ICP preconcentrator

The filter paper and Parafilm were laminated together and sandwiched by glass slides and clamps. When placed in oven at 95 °C for 5 min, the Parafilm melted gradually and penetrated into the filter paper. The penetration depth was controlled by the heating time. Figure 4(A) depicts a representative cross-sectional view of the filter paper embedded by Parafilm after heating. It can be seen that the Parafilm partially penetrated into the filter paper. Following the same workflow (figures 2(A) and (B)), the hydrophobic barriers were formed after direct spraying. Nafion perfluorinated ion exchange resin (Sigma-Aldrich) was pipetted on the centre of the hydrophilic channel to form the permselective membrane. The device was placed on hotplate to evaporate the solvents of the fresh resin at 90 °C.

The schematic of ICP preconcentrator is shown (figure 5(A)). To operate the device, two copper electrodes were

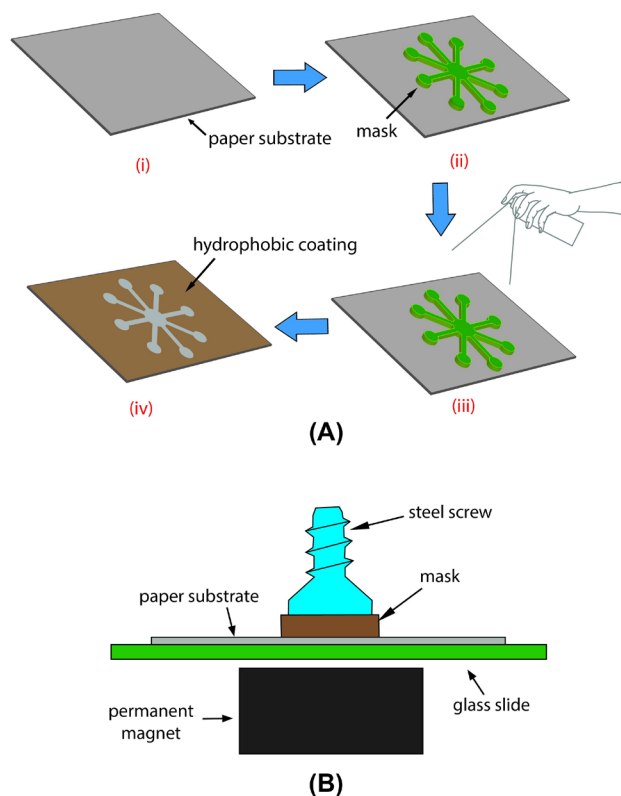


Figure 2. (A) Schematic illustration of the mask-assisted hydrophobic spraying process. (i) Paper substrate was adopted without any pretreatment. (ii) Paper substrate (filter paper or membrane filter) was covered by a mask. (iii) Hydrophobic substance was evenly sprayed onto the substrate. (iv) The desired patterns were obtained after disassembling the mask from the paper substrate. (B) The sandwiched structure with the implementation of magnetic force (not to scale).

placed at the two ends of the channels and a voltage was applied to trigger ion depletion at the anodic side of the Nafion membrane. A DC power supply (PLH250-P, Aim and Thurlby Thandar Instruments, UK) was used to provide 50 V voltage for ICP. Negatively charged FITC with concentration of 20 μM was chosen as fluorescent tracer. NaOH solution with concentration of 100 mM was used to pre-wet the paper channel. The fluorescent tracer movement was observed using an inverted fluorescence microscope (Nikon Eclipse Ti-S) interfaced with a CCD camera (Nikon DS-Ri2). A customized Python program was used to analyse the fluorescence intensity.

2.3. Fabrication of paper-based mSC

The paper-like membrane filter (Shanghai Xinya Purification Instruments) was used as mSC substrate. The paper-based mSC fabrication procedures were schematically illustrated (figures 6(i)–(v)). Firstly, an interdigital pattern was formed on a paper substrate using the same hydrophobic coating approach demonstrated in figure 2. Secondly, the paper substrate was placed at the bottom of a funnel and multi-wall carbon nanotubes (MWCNT)-dispersed solution with concentration of 2 g L⁻¹ in water (Nink-1000, NanoLab, Inc., MA) was infused to the funnel. Then the vacuum pump connected with the funnel was turned on to suck the aqueous

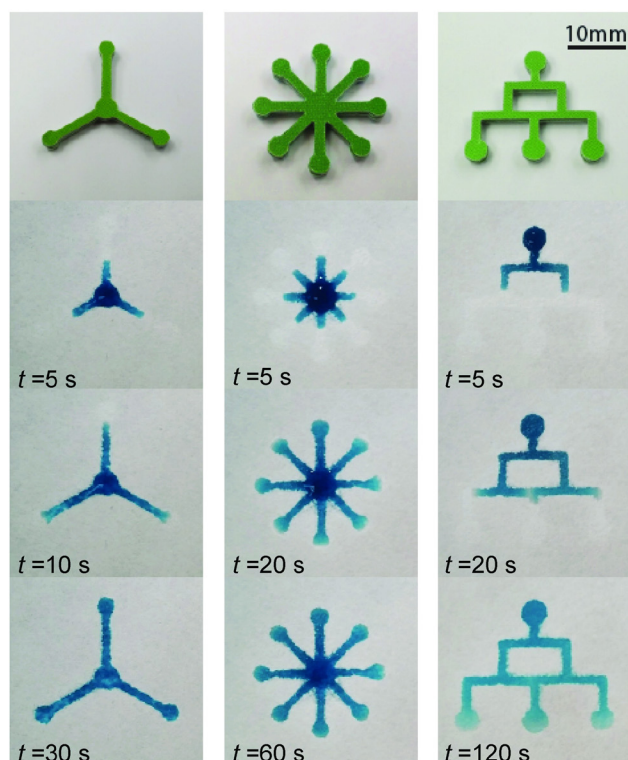


Figure 3. Non-metal masks were applied to fabricate fluidic patterns by using direct spraying method. The masks were made out of inexpensive paperboard. The feasibility of the fabricated fluidic device was demonstrated by the time sequential images of blue dye flowing through the channels.

solution, resulting in the solution flow through the paper substrate. Because the size of MWCNT was larger than that of membrane pore, almost all MWCNT were trapped by the membrane filter and the liquid was drawn through the funnel into the flask below by the vacuum suction force. In addition, due to the water-repellent property of the hydrophobic coating, the solution could only flow through the uncoated parts of the paper substrate. Therefore, MWCNT only filled the hydrophilic parts, remaining the hydrophobic parts clean (figure 6(ii)). The un-deposited areas worked as spacers to separate adjacent electrodes. The closely spaced electrodes gave rise to short ion and electron diffusion pathways. Figure 6(ii) shows the results before and after filtration of MWCNT-dispersed solution. A corresponding video can be found in the supplementary data, found online at (stacks.iop.org/JMM/27/104001/mmedia). The deposited patterns immediately shaped after the filtration. The extra margins of the substrate were then cut off by a scissor, to ensure that the anode and cathode were separated. Sufficient PVA/H₂SO₄ solution was drop-casted onto the paper substrate and dried to form a solid electrolyte (figure 6(iv)). Finally, silver paint was applied to the common areas of the electrodes to glue two separate copper tapes to the electrodes. The conductive copper tapes were used as the extension of the electrodes to connect to an electrochemical workstation for measurements (figure 6(v)). The use of gel electrolyte simplified the formation of a compact micrometer-sized device without the complication of a liquid electrolyte [22].

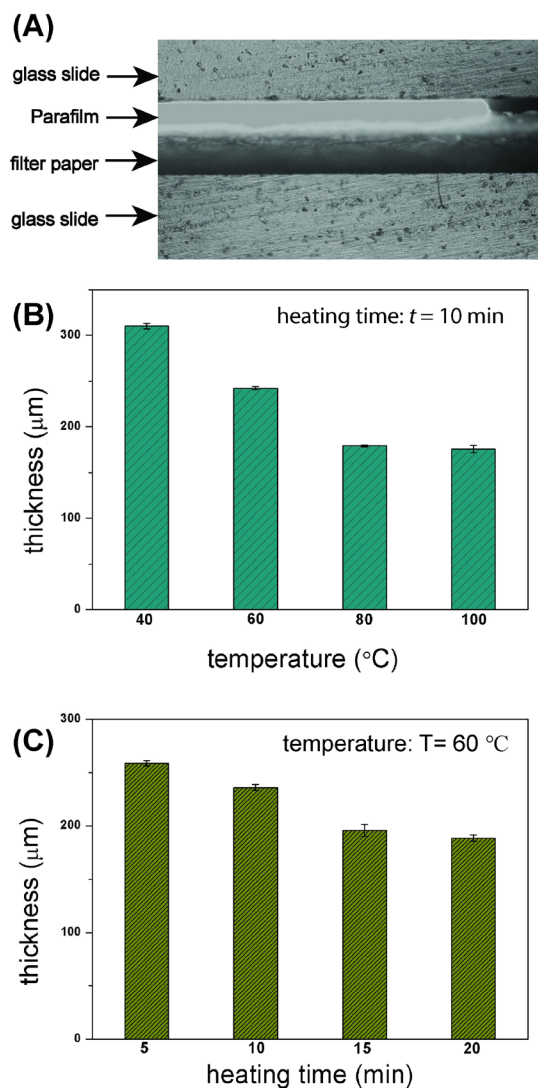


Figure 4. (A) A cross-sectional micrograph of a Parafilm embedded filter paper. The total thickness of Parafilm and filter paper changed as a function of (B) temperature and (C) heating time. Each thickness value is averaged over $N = 5$ measurements.

3. Results and discussion

3.1. Direct spray hydrophobic patterning

Filter paper can absorb a liquid material by capillary action due to the chemical composition and micron-sized structure of cellulose fibres. Micropatterns that are defined through spatially tuning the wettability on filter paper provide an approach to manipulate liquid on paper. Super-hydrophobicity, always referred to as the Lotus effect, has been introduced to industrial and academia applications including microfluidic devices fabrication [23]. The hydrophobic barrier forming is the key procedure for paper-based microfluidic device fabrication. Here we coated paper substrates with commercial hydrophobic material, converting the substrates from hydrophilic to hydrophobic. We achieved spatially selective hydrophobic coating by using masks covered on the substrates. Neverwet[®] is a commercially available water repellent coating that contains organic solvent, including acetone, xylene, and liquefied

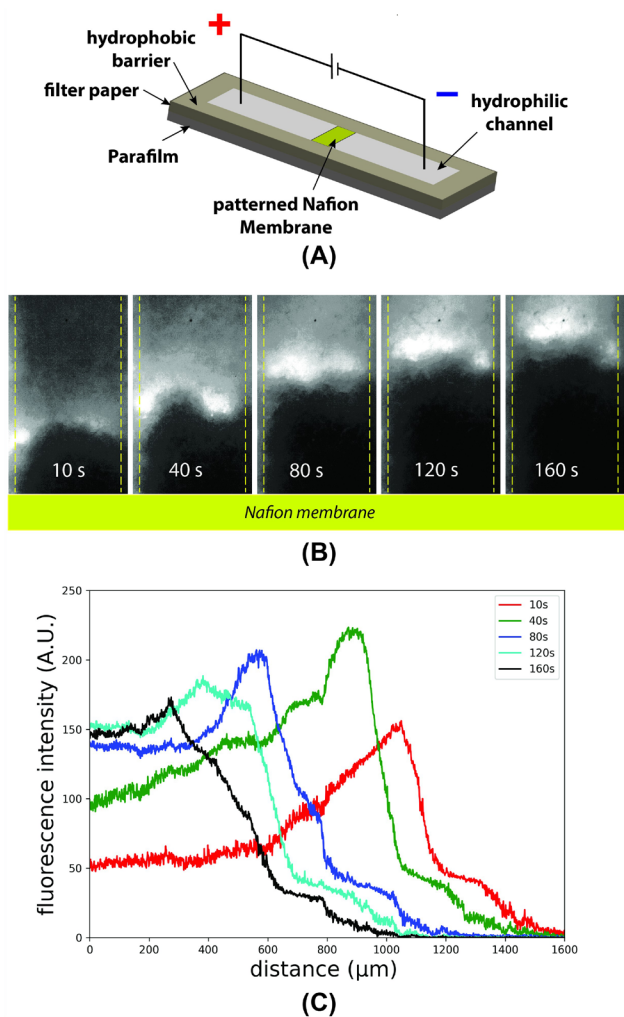


Figure 5. Demonstration of ICP phenomenon in the leak-free μ PAD. (A) Schematic illustration of the paper-based ICP preconcentrator. A hybrid substrate was fabricated through embedding Parafilm into filter paper. The hydrophobic barrier was constructed through direct hydrophobic spraying on the hybrid substrate. (B) Representative images of fluorescent tracer at selected time points. The dashed lines indicate the boundaries of hydrophilic channel. (C) Fluorescence intensity profiles corresponding to above time sequential images.

petroleum gas. Liu *et al* have proved the biocompatibility of the Neverwet[®] treated surface through a series of testing [14]. The coated surface features micro-/nano-scale hierarchical structure that converts the surface from hydrophilic to hydrophobic. A scanning electronic microscope (SEM) (JSM-6700F, JEOL, Japan) was used to analyse the surface features of the paper substrates. An atomic force microscope (AFM) (Dimension SPM, Bruker) was used to probe the 3D morphology of filter paper substrates with and without hydrophobic coating. Images were collected in tapping mode with a cantilever with nominal spring constant of 40 N m^{-1} (Tap 300, Budgetsensors). Hydrophobicity of the treated substrates was characterized by water contact angle measurement. The pristine surface is shown in figure 7(A). The SEM image and AFM 3D morphology of filter paper surface after hydrophobic spraying coating are shown in figures 7(B) and (C). AFM topography shows a roughness $R_q = 441 \text{ nm}$ for hydrophobic

coating area. These morphology pictures revealed that micro-/nano-scale hierarchical structures have been introduced on the filter paper surface by spraying coating, resulting in the cellulose fibres to be fully covered. The hydrophobic feature of the coated substrates is apparent by the water contact angle measurement. Figure 7(D) shows a drop of water maintained almost spherical shape on the hydrophobic substrate, with a contact angle of larger than 120° , indicating that the spraying treatment had converted the paper surface from hydrophilic to hydrophobic.

In order to obtain regular patterns, it is necessary to prevent the diffusion of the sprayed substance into the underneath of the masks. During our experiment, we found that a soft mask was not able to attach to the paper substrate tightly. Hence, some parts of the substrates underneath the mask boundaries were invaded by the sprayed substance, which would break the uniformity of the desired patterns. Two factors are critical for the control of the hydrophobic patterns. First, the mask should be sufficiently rigid to avoid deformation during spraying. Second, the mask should be tightly stacked onto the paper substrate so as to minimise coating substance invasion. In the work reported by Thara *et al*, before conducting spray-on coating, iron mask, which was produced by laser cutting, was attached on top of the paper substrate via magnetic force with a magnetic plate [15]. Here, we propose a method to further simplify the process of stabilizing the mask. After sandwiching paper substrate with mask and glass slide, a permanent magnet was placed behind the glass and some small stainless steel screws on top of the mask. The small screws were forced to stack the mask to the filter paper. The side-view of the stacking was shown in figure 2(B). This process allowed the mask to be non-metal, which is generally easier to fabricate. The minimum channel width is determined by the mask and lateral diffusion effect. In our experiment, we can fabricate channel mask with a minimum width of $500 \mu\text{m}$. To ensure the mask structure were free from any obstruction, only small screws were used on the top of the mask.

CNC milling was carried out for the fabrication of the mask, where hard acrylic materials were used to mask the substrates efficiently. We also demonstrated that the similar pattern can be formed by using craft cutter on a discarded paperboard. Then, 6 piece of similar masks were laminated together with glue. The stiffness of the laminated paperboard mask was comparable to that of an acrylic mask. Therefore, the laminated paper mask can be used in the spraying coating fabrication.

Figure 3 shows the representative as-fabricated paper-based microfluidic chips and adopted masks. The hydrophilic channels were stained by blue dye for visualization and captured at different time points. The minimum width of the channels was 1 mm . It can be seen from the image that with the increase of total channel area and complexity, the colour dye required more time to fully wet all hydrophilic channels. As shown in the images, the fabricated channels look slightly smaller than the masks, and the edges of the channels look a little rough. In the spraying process, the sprayed aqueous hydrophobic materials randomly fell on the paper substrate, resulting in uneven distribution of the hydrophobic materials on the surface. This unevenness was obvious at the edges of the channel and led

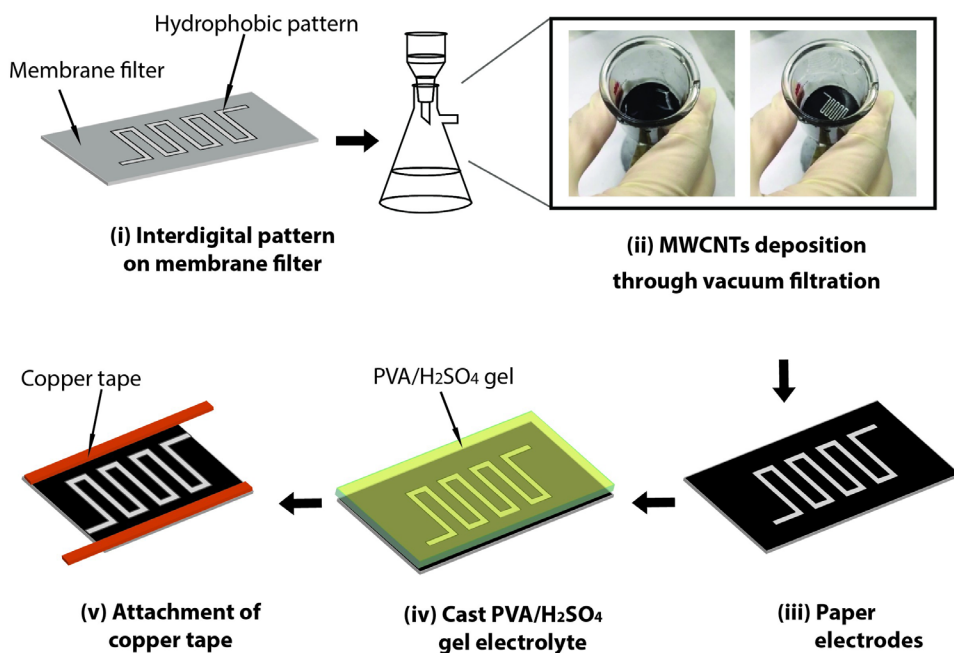


Figure 6. Schematic fabrication of paper-based mSC based on hydrophobic spraying: (i) interdigital electrodes pattern was fabricated through spraying hydrophobic coating on membrane filter. (ii) Vacuum filtration technique was utilized to deposit conductive MWCNTs onto the uncoated part of the membrane filter (inset: before vacuum suction, the membrane filter was submerged by carbon solution (left), interdigital electrodes appeared on the membrane filter after vacuum suction (right)). (iii) The cartoon of as-fabricated planar carbon electrodes on paper substrate. (iv) Drop-casting of PVA/H₂SO₄ gel electrolyte onto the planar electrodes on paper substrate. (v) Attachment of copper tape to cathodic and anodic electrodes for electrical connection.

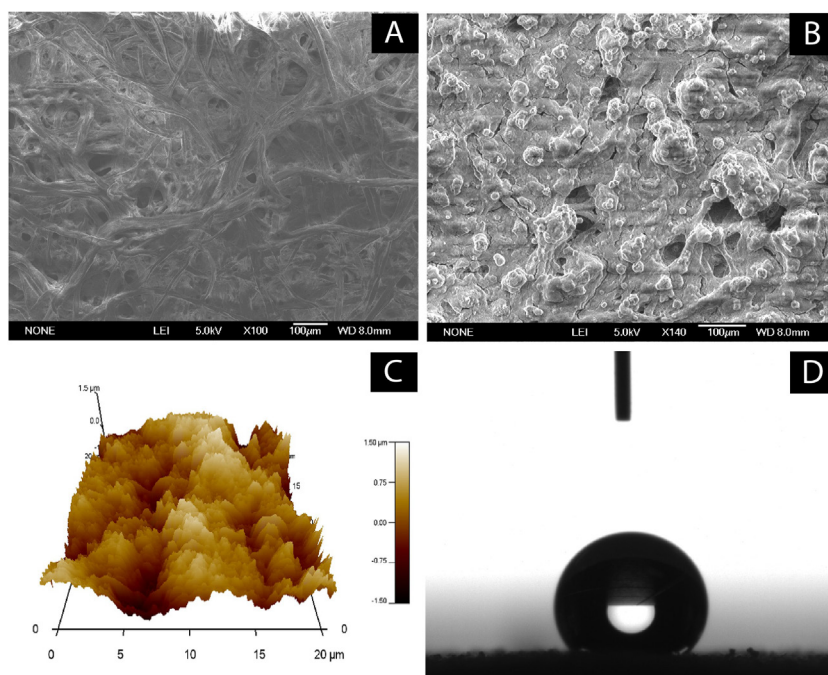


Figure 7. Surface characterization of paper substrates. SEM images of Whatman[®] grade 1 filter paper (A) before and (B) after hydrophobic coating; (C) AFM 3D morphology of filter paper after hydrophobic coating; (D) water contact angle measurement on filter paper after hydrophobic coating.

to the irregularity of the channel edges. Figure 8 shows the microscopic views of the channels fabricated on filter paper substrate. It can be clearly seen that the boundaries between the hydrophobic region and the hydrophilic region are not very uniform, which is a common phenomenon for most paper-based microfluidic devices.

In the spraying process, the spray depth and lateral diffusion of the hydrophobic materials are two important factors, which can influence the channel profile. The spraying depth relies on spraying time and the distance between spraying nozzle and the substrate. To ensure that the hydrophobic materials can penetrate through the entire thickness of the paper

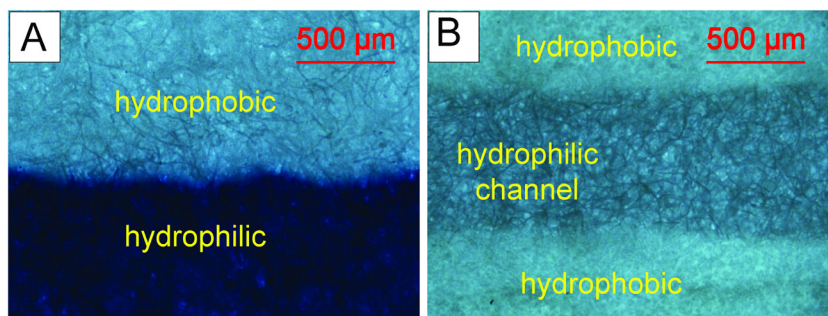


Figure 8. The microscopic views of paper-based microfluidic channels observed by optical microscope at $4\times$ magnification. (A) The boundary between hydrophobic coating (top) and hydrophilic paper channel soaked with blue food dye (bottom). (B) A hydrophilic channel defined by hydrophobic coating.

substrate, the substrates were sprayed for 3 s with a distance between spraying nozzle and the substrate of around 15 cm. Lateral diffusion is another factor that should be considered. Due to the diffusion, the hydrophobic materials can propagate to the covered area from the side of the mask within the paper, resulting in around 10% variation of the dimensions of the fabricated channel from the mask.

3.2. Leak-free paper-based ICP preconcentrator for fluorescence sensing

The μ PADs fabricated using wax printing contains channels for the entire thickness of the paper. Consequently, when liquid samples are loaded in the device, the device must be suspended in air to avoid direct contact with other surfaces, which may induce sample contamination or loss. Parafilm is one of the mostly used laboratory consumables with high biocompatibility and chemical inertness. It can melt at above $60\text{ }^{\circ}\text{C}$ due to paraffin wax property. Direct hydrophobic spraying combining with Parafilm embedding provides an easy-to-use approach to fabricate μ PADs, albeit not yet fully reported so far. The microfluidic devices fabricated by this hybrid technique are expected to have the following advantages: (1) the Parafilm seals the paper bottom, providing a flexible and strong support for the device, and the paper device can be placed on a solid surface, such as glass slide. These increase operation versatility whilst reduce the contamination risk; (2) a shallow channel can be achieved through the Parafilm embedding, enabling rapid heat dissipation and reduced sample consumption during ICP process.

To determine the heating temperature and time applied for Parafilm embedding, the entire thickness of Parafilm-filter paper composite was measured under different conditions. The variation of entire thickness of Parafilm-filter paper hybrid structure with temperature and heating time are shown in figures 4(B) and (C) respectively. Initially, the entire thickness of the hybrid structure was around $310\text{ }\mu\text{m}$. Figure 4(B) shows the thickness changes when the Parafilm-filter paper composites were left at different temperatures for 10 min. The thickness did not change when the heating temperature was set at $40\text{ }^{\circ}\text{C}$, indicating the Parafilm did not melt. When the temperature was set above $60\text{ }^{\circ}\text{C}$, during a same period, more Parafilm penetrated into the filter paper with increased temperature, resulting in reduced entire thickness. Figure 4(C) shows that at the same temperature ($T = 60\text{ }^{\circ}\text{C}$) the entire thickness

decreased gradually with time, suggesting that more Parafilm melted with time. When the Parafilm was embedded at $100\text{ }^{\circ}\text{C}$ for 10 min, the entire thickness decreased to the thickness of the original filter paper ($180\text{ }\mu\text{m}$).

To demonstrate the practical feasibility of the Parafilm embedded μ PAD, a sample preconcentration and sensing experiment based on ICP effect was performed on this μ PAD. The ICP experiment was carried out on the μ PAD under the applied voltage of 50 V. The device was first pre-wetted by 100 mM NaOH solution, followed by dropping $20\text{ }\mu\text{l}$ FITC tracer with concentration of 20 mM. Fluorescent images were recorded every 10 s for subsequent analysis. Experiment results for fluorescent tracer depletion and concentration are shown in figures 5(B) and (C). As demonstrated in figure 5(B), ion depletion region generated within 10 s after electric field applied and continuously expanded. Due to the presence of negatively charged sulfonic acid groups in Nafion, only cations can transport through the Nafion membrane that contains nanopores. At the anodic side of the permselective membrane, the ion depletion band formed shortly after applying voltage as a result of initial electroosmotic flow (EOF), which driven the negatively charge fluorescent tracer move toward the cathodic direction. In the depletion region, the electrophoretic migration (EPH) is dominant, pushing the fluorescent tracer toward the anodic side. The balance of the two opposing effects resulted in ions focused at the depletion boundary [24]. With time passed, the depletion band extended and more fluorescent ions concentrated at the depletion boundary, forming a preconcentration plug.

The fluorescence intensity profiles at some selected time points corresponding to figure 5(B) are plotted in figure 5(C). To quantify the preconcentration performance, the ratio of maximum to initial fluorescence intensity was used as the preconcentration factor. The measured maximum preconcentration factor reached up to 220-fold at 40 s. During the experiment, we observed that the maximum concentration decreased after 40 s. This can be attributed to the evaporation effect, including natural evaporation and Joule heating induced evaporation [18].

3.3. Paper-based microsupercapacitors

Direct spraying method also provides an alternative way to fabricate in-plane mSCs by patterning the carbon nanotubes (CNTs) on the surface of film substrate. In order to exploit the

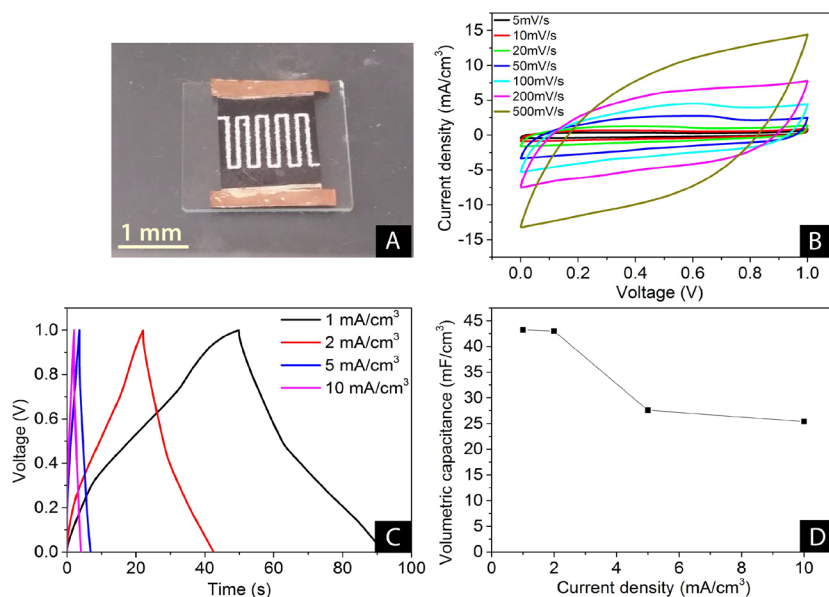


Figure 9. Performance of the fabricated micro-supercapacitors. (A) The photograph of as-fabricated mSC. (B) Cyclic voltammetry (CV) curves of mSCs at different scan rates from 5–500 mV s^{-1} . (C) Galvanostatic charge-discharge (GCD) curves of mSC at various charge/discharge rates. (D) Rate capabilities of mSCs.

potential of direct spraying hydrophobic patterning method, membrane filter was utilized as mSC substrate and vacuum filtration technique was used to deposit electrodes on the substrate [25]. The filter, which is paper-like membrane, is used for filtering aqueous solutions and can retain particles or microorganisms that are larger than membrane pore size. The paper-like membrane filter was chosen as mSC substrate for two reasons: (1) it possesses high flexibility, solvent compatibility, and hydrophilicity. These properties are similar to filter paper that are commonly used as μPADs substrates; (2) its high pore density and narrow pore size distribution ensure a high-level particle retaining. Vacuum filtration is a widely used technique for separating solid product from a mixture of solid and liquid. The objective here was to use this technique to deposit conductive materials onto the membrane filter that bears primary interdigital electrodes pattern.

Figure 6 shows three steps to fabricate conductive electrodes on paper: (1) hydrophobic patterning, (2) vacuum filtration and (3) packing. As illustrated above, the mask assisted spraying coating method provided a fast hydrophobic patterning approach. Vacuum filtration technique was adopted to deposit conductive materials onto the membrane filter, on which the interdigital electrodes pattern was formed beforehand. The unique micro-architectures of membrane filter with porous structure allows water pass through while retaining substance with certain dimensions. Carbon materials such as carbon nanotubes (CNTs) and graphene could be absorbed into paper membrane filter, rendering its conductivity and even electrochemical activity. Vacuum filtration process can be completed in several minutes, and a conductive membrane is achieved by simply soaking the solutions containing carbon materials. On the paper-based mSC, the electrodes should be highly conductive to work as current collector. As CNTs have been widely accepted for SCs applications, we chose CNTs as conductive material to construct interdigital electrodes.

In the case of in-plane paper-based mSC, the interdigital electrodes on paper substrates are the central parts of the mSC architecture. Figure 9(A) shows the configuration of the interdigitated electrodes. The length of each electrode was 10 mm and the width was 500 μm . The spacing between two neighbouring electrodes was 500 μm . The subsequent electrochemical performance characterization was mainly conducted on the electrodes basis.

A parametric study was conducted by measuring cyclic voltammetry (CV), galvanostatic charge-discharge (GCD), and electrochemical impedance spectroscopy (EIS) in a three-electrode configuration (figures 9(B)–(D)). The cycling performance of this in-plane supercapacitor was tested at different scan rates from 5–500 mV s^{-1} (figure 9(B)). In the voltage window ranging from 0–1.0 V, the CV curves exhibited nearly rectangular shapes, demonstrating the effective formation of an electric double layer (EDL) at the electrode/electrolyte interface and good charge propagation across the electrodes. Furthermore, as the scan rate increased above 100 mV s^{-1} , the voltammograms window tended to tilt toward the vertical axis, thereby becoming a quasi-rectangle. This result indicated the dominance of the double layer formation in the energy storage process at lower scan rates.

The calculated areal capacitance of our supercapacitor was 0.32 mF cm^{-2} at 10 mV s^{-1} scan rate, which was in accord with many previous reports of carbon-based all-solid-state supercapacitors. Li *et al* fabricated an in-plane microsupercapacitor using silver nanoparticles as current collectors and obtained 0.59 mF cm^{-2} areal capacitance at 100 mV s^{-1} scan rate [26]. Based on the same printing technique, they constructed all-solid-state graphene-based in-plane microsupercapacitors with interdigitated structure on silicon wafers. The devices showed areal capacitance over 0.14 mF cm^{-2} at 5 mV s^{-1} scan rate [27]. Notarianni *et al* presented a flexible thin film supercapacitor, which achieved areal capacitance of 0.4

mF cm⁻² at 10 mV s⁻¹ scan rate [28]. The performance of our supercapacitor is comparable to these studies.

Figure 9(C) shows the GCD curves of the devices at different current densities, which was used to further understand the capacitive features of the mSC. The symmetric triangular-shaped GCD curves with a nearly linear variation of voltage as a function of time during charge and discharge can be observed. Both the symmetry and good linear profile of the charge and discharge curves indicated the good capacitive performance of the device. Correspondingly, the volumetric capacitance was calculated to be 42.5 mF cm⁻³ at a current density of 2 mA cm⁻³ (figure 9(D)).

Fabrication of paper-based mSC suggested feasibility and versatility of this proposed hydrophobic patterning method. Compared with the photolithography and related fabrication methods, our approach simplified fabrication process by utilizing manual hydrophobic patterning and vacuum filtration. This approach provides an alternative route to achieve the same device for researchers with limited lab resources. One of the most promising applications of the as-proposed paper mSC is integration of on-chip battery to build a self-powered microfluidic sensor. This integration shall miniaturize the microfluidic system by replacing the bulky external power supplies. As the membrane filter possesses the similar properties as those of filter paper, a μ PAD can be co-fabricated on the same filter membrane substrate.

4. Conclusions

In this work, we demonstrated a simple spraying method to fabricate paper-based microfluidic devices. The fluidic channels on paper were formed through one-step mask assisted hydrophobic spraying. Compared with traditional μ PADs fabrication methods such as wax-printing and photolithography, this direct spraying approach does not require complex facilities. Based on this hydrophobic patterning technique, we further developed two hybrid methods to fabricate functional microdevices: a leak-free ICP preconcentrator for fluorescence sensing, and a paper-based mSC. The versatility of this patterning approach opens up new routes to prototype highly integrated, paper-based microfluidic sensors.

Acknowledgments

This work was supported by the Singapore National Research Foundation, Prime Minister's Office, under a Competitive Research Programme (Non-volatile Magnetic Logic and Memory Integrated Circuit Devices, NRF-CRP9-2011-01), and an Industry-IHL Partnership Program (NRF2015-IIP001-001). WSL is a member of the Singapore Spintronics Consortium (SG-SPIN). The support from an RIE2020 AME-Programmatic Grant (No. A1687b0033) is also acknowledged.

ORCID iDs

Ning Liu  <https://orcid.org/0000-0002-9549-3375>

References

- [1] Martinez A W, Phillips S T, Butte M J and Whitesides G M 2007 Patterned paper as a platform for inexpensive, low-volume, portable bioassays *Angew. Chem., Int. Ed.* **46** 1318–20
- [2] Sackmann E K, Fulton A L and Beebe D J 2014 The present and future role of microfluidics in biomedical research *Nature* **507** 181–9
- [3] Yetisen A K, Akram M S and Lowe C R 2013 Paper-based microfluidic point-of-care diagnostic devices *Lab Chip* **13** 2210–51
- [4] Cate D M, Adkins J A, Mettakoonpitak J and Henry C S 2015 Recent developments in paper-based microfluidic devices *Anal. Chem.* **87** 19–41
- [5] Li X, Ballerini D R and Shen W 2012 A perspective on paper-based microfluidics: current status and future trends *Biomicrofluidics* **6** 11301–113
- [6] Xia Y Y, Si J and Li Z Y 2016 Fabrication techniques for microfluidic paper-based analytical devices and their applications for biological testing: a review *Biosens. Bioelectron.* **77** 774–89
- [7] Coltro W K T, de Jesus D P, da Silva J A F, do Lago C L and Carrilho E 2010 Toner and paper-based fabrication techniques for microfluidic applications *Electrophoresis* **31** 2487–98
- [8] Carrilho E, Martinez A W and Whitesides G M 2009 Understanding wax printing: a simple micropatterning process for paper-based microfluidics *Anal. Chem.* **81** 7091–5
- [9] Nie J F, Liang Y Z, Zhang Y, Le S W, Li D N and Zhang S B 2013 One-step patterning of hollow microstructures in paper by laser cutting to create microfluidic analytical devices *Analyst* **138** 671–6
- [10] Phan D T, Shaegh S A M, Yang C and Nguyen N T 2016 Sample concentration in a microfluidic paper-based analytical device using ion concentration polarization *Sensors Actuators B* **222** 735–40
- [11] Olkkonen J, Lehtinen K and Erho T 2010 Flexographically printed fluidic structures in paper *Anal. Chem.* **82** 10246–50
- [12] Yu L and Shi Z Z 2015 Microfluidic paper-based analytical devices fabricated by low-cost photolithography and embossing of Parafilm (R) *Lab Chip* **15** 1642–5
- [13] Hancock M J, He J K, Mano J F and Khademhosseini A 2011 Surface-tension-driven gradient generation in a fluid stripe for bench-top and microwell applications *Small* **7** 892–901
- [14] Liu C C et al 2016 A high-efficiency superhydrophobic plasma separator *Lab Chip* **16** 553–60
- [15] Nurak T, Praphairaksit N and Chailapakul O 2013 Fabrication of paper-based devices by lacquer spraying method for the determination of nickel (II) ion in waste water *Talanta* **114** 291–6
- [16] Wong S R Y, Cabodi M, Rolland J and Klapperich C M 2014 Evaporative concentration on a paper-based device to concentrate analytes in a biological fluid *Anal. Chem.* **86** 11981–5
- [17] Gong M M, Nosrati R, Gabriel M C S, Zini A and Sinton D 2015 Direct DNA analysis with paper-based ion concentration polarization *J. Am. Chem. Soc.* **137** 13913–9
- [18] Yang R J, Pu H H and Wang H L 2015 Ion concentration polarization on paper-based microfluidic devices and its application to preconcentrate dilute sample solutions *Biomicrofluidics* **9** 014122
- [19] Han S I, Hwang K S, Kwak R and Lee J H 2016 Microfluidic paper-based biomolecule preconcentrator based on ion concentration polarization *Lab Chip* **16** 2219–27
- [20] Yeh S H, Chou K H and Yang R J 2016 Sample pre-concentration with high enrichment factors at a fixed

- location in paper-based microfluidic devices *Lab Chip* **16** 925–31
- [21] Ge L *et al* 2013 Photoelectrochemical lab-on-paper device based on an integrated paper supercapacitor and internal light source *Anal. Chem.* **85** 3961–70
- [22] Kim S K, Koo H J, Lee A and Braun P V 2014 Selective wetting-induced micro-electrode patterning for flexible micro-supercapacitors *Adv. Mater.* **26** 5108–112
- [23] Xing S Y, Jiang J and Pan T R 2013 Interfacial microfluidic transport on micropatterned superhydrophobic textile *Lab Chip* **13** 1937–47
- [24] Gong M M, Zhang P, MacDonald B D and Sinton D 2014 Nanoporous membranes enable concentration and transport in fully wet paper-based assays *Anal. Chem.* **86** 8090–7
- [25] Ma C W, Huang P C and Yang Y J 2015 A paper-like micro-supercapacitor with patterned buckypaper electrodes using a novel vacuum filtration technique *Proc. IEEE Conf. on Micro Electro Mechanical Systems (MEMS)* pp 1067–70
- [26] Li J T, Ye F, Vaziri S, Muhammed M, Lemme M C and Ostling M 2013 Efficient inkjet printing of graphene *Adv. Mater.* **25** 3985–92
- [27] Li J T, Mishukova V and Ostling M 2016 All-solid-state micro-supercapacitors based on inkjet printed graphene electrodes *Appl. Phys. Lett.* **109** 123901
- [28] Notarianni M, Liu J Z, Mirri F, Pasquali M and Motta N 2014 Graphene-based supercapacitor with carbon nanotube film as highly efficient current collector *Nanotechnology* **25** 435405